Turkish Journal of Electrical Engineering & Computer Sciences

http://journals.tubitak.gov.tr/elektrik/

Research Article

Turk J Elec Eng & Comp Sci
(2016) 24: 4670 – 4681

doi:10.3906/elk-1501-15

Sinusoidal current injection based on a line-commutated inverter for single-phase grid-connected renewable energy sources

Murat ÜNLÜ*, Sabri ÇAMUR, Ersoy BEŞER, Birol ARİFOĞLU
Department of Electrical Engineering, Faculty of Engineering, Kocaeli University, Kocaeli, Turkey

Received: 03.01.2015 • **Accepted/Published Online:** 25.08.2015 • **Final Version:** 06.12.2016

Abstract: This paper presents a new power electronic interface based line-commutated inverter (LCI) for dc power injection to the grid. The proposed system involves a simple power electronic converter and controller interface using a single-phase LCI. The controller has been developed that can inject a high quality sinusoidal current to the utility grid from the dc source. By this means, ac side harmonic filters and the harmonic cancellation technique are eliminated.

The proposed system facilitates controlling the injected current with a controllable power factor of operation. The complete system has been modeled in MATLAB/Simulink and tested experimentally with the laboratory prototype. Finally, the simulation and the experimental results show good performance of the proposed LCI technique. The total harmonic distortion (THD) of the injected currents for the different power factors and reference current signals is achieved less than 5%, which meets the grid-connected standards. The proposed single-phase LCI inverter system is a good alternative to the dc power transfer from renewable energy sources (photovoltaic, fuel cell etc.) to the utility grid.

Key words: Line-commutated inverter, sinusoidal current, grid-connected, renewable energy sources, total harmonic distortion

1. Introduction

The development in renewable energy sources replaces the other traditional energy sources such as the fossil- and nuclear-based generation. A power electronic interface is required to connect renewable energy sources such as photovoltaic, wind, and fuel cells to the utility grid [1]. In the past, most houses with solar electric systems were not connected to the local grid utility. In recent years, however, the number of houses having PV systems connected to the utility grid has increased significantly. The grid-connected PV systems can transfer generated the dc power directly to the utility system; consequently it usually does not require a battery bank to store energy in contrast to stand-alone PV systems [2]. This is accomplished by means of grid-connected inverters. Therefore, power transfer to the utility grid is becoming more of an issue and more visible and inverter technology has dramatically improved during the last decade [3]. The main function of an inverter interfacing PV module for grid-connected applications is to convert the dc input current obtained from the PV module to the ac sinusoidal current and inject it into the grid [4]. The inverter must meet stringent technical standards as it injects good-quality sinusoidal current into the grid and must be synchronized with the utility grid [2]. The inverter circuits can be generally classified as voltage-source inverters (VSIs) and current-source inverters (CSIs) [2]. The aim of both the VSI and the CSI is to inject a sinusoidal current into the grid. In the VSI, a

*Correspondence: muratunlu@kocaeli.edu.tr

sinusoidal grid current can be generated by applying positive/negative or zero voltage to the grid inductor. The VSI generates an ac output voltage waveform composed of discrete values; therefore, an inductor filter should be used between the VSI and the grid in order to produce a sinusoidal current waveform. In the CSI, the current is already modulated to track a rectified sinusoidal waveform and the function of the circuit is to re-create the sinusoidal waveform and inject it into the grid [4]. The CSI generates an ac output current waveform composed of discrete values; therefore, a capacitor filter should be used between the CSI and the grid in order to produce a sinusoidal voltage waveform.

Grid-connected inverters can be classified according to their commutation type as line-commutated and self-commutated. The self-commutated inverter computes its turn-on and turn-off timing by using high-frequency switching devices such as MOSFETs and IGBTs [3]. It is composed of an H-bridge and uses pulse-width modulated (PWM) switching control to shape sinusoidal current and so is switched at high frequencies (>16 kHz) [5]. It is for this reason that the total losses of the inverter are more with respect to the line-commutated inverters. However, apart from higher switching losses, the forward voltage drop of the IGBTs on the market is higher than in comparison to the same ratings SCRs and thus the power transfer capability of the LCI is quite high with respect to MOSFET/IGBT [6]. Consequently, the LCI inverter would be more efficient than the self-commutated inverter, which is composed of IGBT and MOSFET particularly in higher power ratings. In contrast to self-commutated inverters, line-commutated inverters (naturally commutated converters) do not need to compute turn-off timing switching devices that can only be forced turn-on because the LCI is realized by means of silicon-controlled rectifiers (SCRs). Therefore, while one SCR is turned on, it cannot be turned off unless the current flowing in is zero; turning on another SCR only forces to its current to be zero.

The line-commutated inverters were based on technologies used in electrical drives from the beginning of the 1980s and generally used for electric-motor applications [2]. The line-commutated inverters are available with power ratings of 1.5 kVA [7]. The LCI is equipped with four SCRs for a single-phase system. It can be used in power transfer for grid connected small-distributed power generation systems like a PV or fuel cell. The major advantages are having a simple structure, high efficiency, cheapness, and robustness. In addition to the advantages of this inverter, it is automatically synchronized with the utility grid thanks to the native advantage of self-latching property of SCRs as being operated as line commutated. This feature is possible only with SCR converters. However, lower power factor and containing harmonics in the injecting current were major drawbacks [7]. Tuned filters need to be employed to suppress these harmonics.

The basic circuit diagram for a single-phase LCI is shown in Figure 1. In this circuit, when the firing angle α is between $90^\circ < \alpha < 180^\circ$, the average output voltage of fully controlled SCR bridge V_d becomes positive, which is computed as given in Eq. (1). In this case, the converter operates as a line-commutated inverter. When the load is a dc source, the direction of power flow can reverse and so the power can be transferred from the dc source to the grid.

$$V_d = \frac{2}{\pi} V_m \cos\alpha \tag{1}$$

where V_m is the peak value of phase voltage of the utility grid and α is the firing angle.

In recent years, some studies performed on LCIs have accomplished power transfer to the grid but they commonly have some drawbacks. The conventional circuit used in these studies is shown in Figure 2, where the dc source is connected to a SCR bridge via an inductor [8]. In previous studies, the injecting current waveform approximates a square wave, where the total harmonic distortion (THD) of output current is fairly high due to

harmonics [9–14]. It is for this reason that the THD of the current would be far higher than that determined by the international standards such as IEEE-1547 and IEC 61727 [6,15]. Consequently, it involves filtering equipment, which results in increasing cost and reduced efficiency. In addition to this drawback, the power factor is not stable in some studies because of where the firing angle α is used in the control signals to track the maximum power point [9,10,12,14].

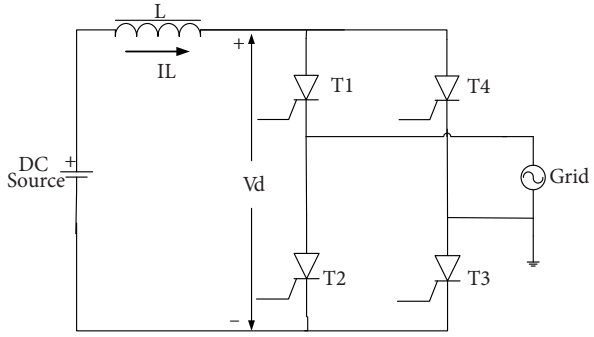

Figure 1. Line-commutated inverter basic circuit.

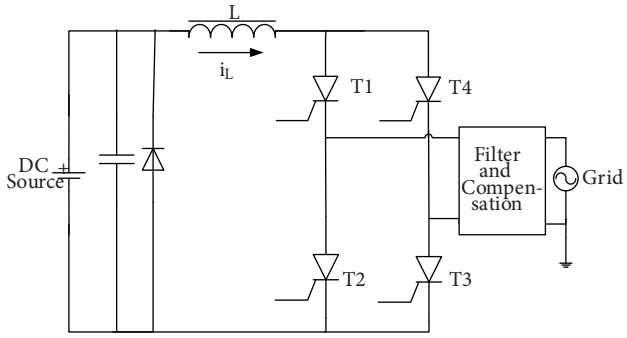

Figure 2. The conventional line-commutated inverter circuit [9].

In this paper, to overcome all the drawbacks of the conventional LCI, a new power electronic interface circuit based on LCI is developed. The proposed circuit is capable of injecting a sinusoidal current with low harmonic contents into the grid at constant power factor. Hence, the THD of injecting current into the grid is reduced, satisfying the grid standards. In addition to injecting sinusoidal current, this circuit also allows using the RMS values of current as control signals instead of the firing angle α. Therefore, the proposed inverter can operate at constant power factor. This topology provides a grid-connected single-phase inverter topology to offer a simple, robust, and low-cost solution. The proposed inverter is a good alternative to connect the PV system to the utility grid. It can be used in renewable applications and it is efficient, particularly the fuel cells and photovoltaic systems, due to its output dc voltage and current.

2. The conventional line-commutated inverter (LCI)

Conventional LCI circuits have been used to deliver the dc power available at PV generators or other renewable sources to the grid. In these methods, a line-commutated full-wave controlled rectifier can be operated in inversion mode by connecting a dc voltage source at the load side and controlling the switching angle (α). Ideally, firing angle α can stretch to 180° for the inversion mode, but practically it should be less than 180° so that the SCR can turn off or commutate. Thus, it is a slightly lagging power factor. However, they have square-shaped grid current that contains high harmonic contents.

2.1. Harmonic analysis of the conventional single-phase LCI

The main drawback of the conventional line-commutated inverter is injecting nonsinusoidal current into the grid. This current is uncontrolled and approximately square wave that includes harmonic components. In this case, the total harmonic distortion of the injecting current (THD_i) can be calculated as in the below equations.

The RMS value of the total current is given by $I_s = I_{srms} = I_d$, and Fourier analysis calculates the RMS value of the fundamental current I_{s1} according to (2)

$$I_{s1} = (a_1 \cos \pi\omega t + b_1 \sin \pi\omega t) \tag{2}$$

$$a_1 = 0, \;\; b_1 = \frac{4I_d}{\pi}, \; I_{s1} = \sqrt{a_1^2 + b_1^2} = \frac{4I_d}{\pi}$$

$$I_{s1rms} = \frac{I_{s1}}{\sqrt{2}} = \frac{2}{\pi}\sqrt{2}I_d = 0.9I_d$$

The THD_i is calculated as given by Eq. (3)

$$THD_i = 100x\sqrt{\frac{I_{srms}^2 - I_{s1rms}^2}{I_{s1rms}^2}} \tag{3}$$

It can be derived from (3) that the THD of the injected current to the grid is obtained quite high as 48.4% for single-phase in the conventional LCI circuit.

3. The proposed single-phase grid-connected LCI system

The proposed single-phase grid-connected LCI circuit and its operating principle with switching intervals are shown in Figures 3 and 4, respectively. The proposed circuit improves the wave shape of the injecting current and hence reduces the total harmonic distortion of the injecting current (THD_i). This scheme of power transfer involves a line-commutated inverter that is composed of four SCRs, a dc-link inductor, a step-up transformer, and a sinusoidal current injection module including two controlled switches (MOSFETs) and two diodes. The sinusoidal current injection module feeds the SCR bridge, which operates as a line-commutated inverter through dc-link inductance.

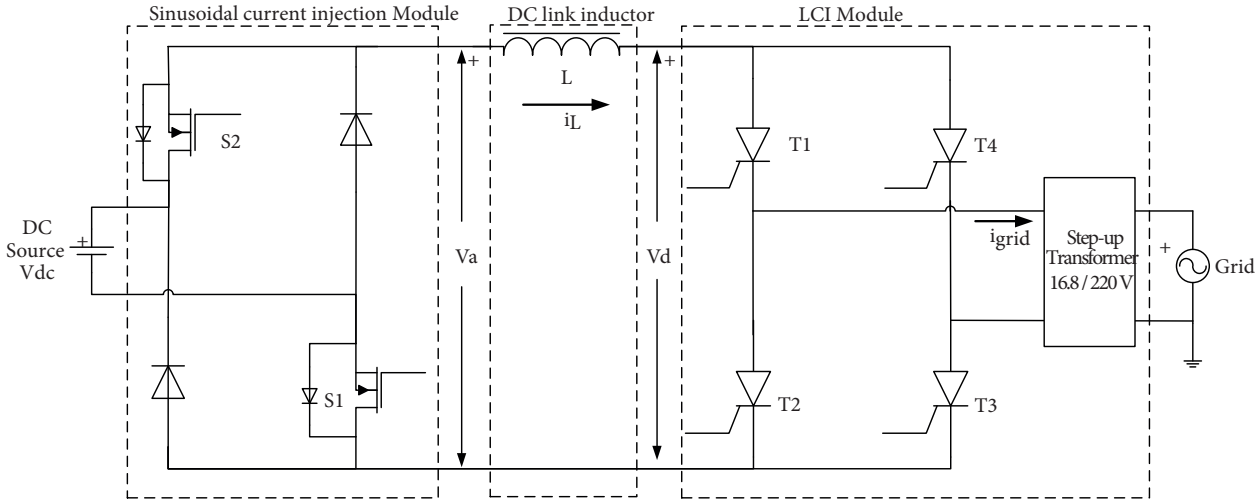

Figure 3. The proposed single-phase grid-connected LCI circuit.

In this study, a step-up transformer is used at the AC side. There are two alternatives to connect to the grid. It can be used a step-up transformer or directly connected to the AC side in the case of having a large dc source at the DC side. The large dc source can be preferred to reduce the number of stages in such systems. Here a step-up transformer is used to allow studying lower power in the laboratory and connected the input of the LCI. In this paper, the inverter output current is shaped into sinusoidal waveform. The firing angle is kept at a constant value for each SCR in a fully controlled SCR bridge. A key component of the inverter

is the controller. It implements the current controller that drives the MOSFETs, provides sinusoidal current complying with grid interface requirements, and generates firing pulses for SCRs.

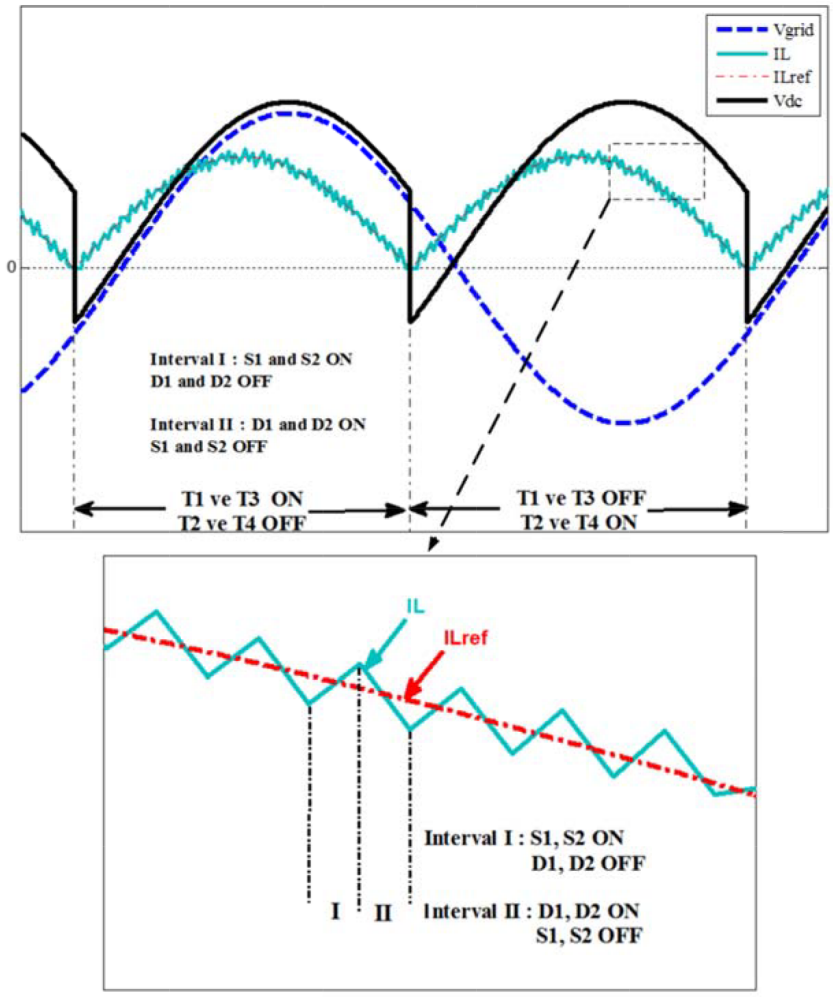

Figure 4. The proposed inverter operating principle with switching intervals (red linereference current generated in the controller, green linethe real current through dc-link inductor by forced proposed controller).

3.1. LCI module

In the proposed scheme the dc source is connected to the grid via a LCI. A fully controlled bridge converter is used in this module. The LCI module is obtained by operating a line-commutated converter in an inverter mode (α >90°). This module contains four SCRs as shown in Figure 3. The circuit components of the LCI module are (T1, T2, T3, T4) SCRs (IXYS CS35) and an MOC3021 optoisolators triac driver is preferred for the SCR trigger circuit. The firing pulses for SCRs are generated in DsPIC30F3011 as a software interrupt and sent to T1, T2, T3, and T4 SCRs via driving and isolation circuit including MOC3021.

3.2. Sinusoidal current injection module

These switches are operated in current-regulated mode at high frequency so that drawing current from (i_L) dc link current is the same as the reference current (i_{Lref}). This reference current is built in the microcontroller

and applied to the hysteresis controller. In this module, the power electronic switches two MOSFETs (S1 and S2) and two power diodes as can be seen in Figure 4. The MOSFETs operate as a waveshaper at high switching frequency. They were driven via a TLP250 optocoupler MOSFET driver circuit according to signals from the controller (DsPIC30F3011).

3.3. Zero crossing detection (ZCD)

The zero-crossing detection (ZCD) and phase locked loop (PLL) techniques are generally used for sensing zero crossings of the grid voltage [16]. Here the ZCD is exploited to obtain a reference signal according to the grid voltage. This reference signal is needed to produce reference inductor current i_{Lref} and compute timing of firing pulses for SCRs as depicted in Figure 4. The fundamental sinusoidal waveform (internal tables) is built in the controller based on ZCD signals. The working of the complete system is summarized with a simplified block diagram of the proposed system with the power electronics in Figure 5. In this study, the hardware interrupt of DsPIC30F3011 is used for ZCD signals so that the accurate reference current signal can be built.

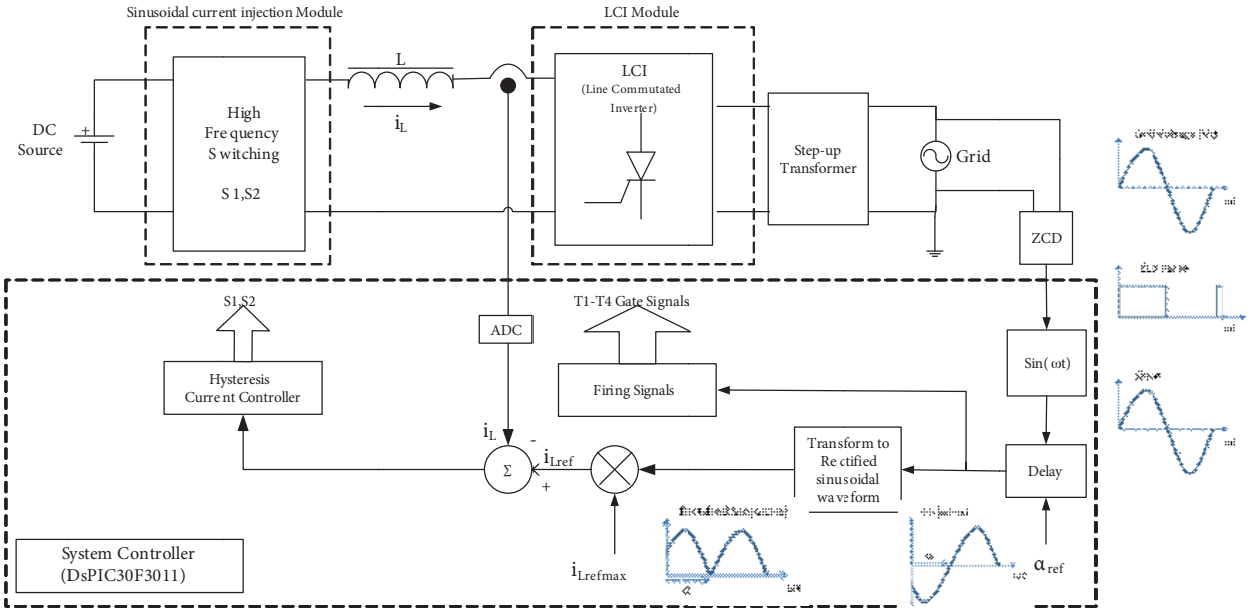

Figure 5. The block diagram of the proposed LCI system scheme.

3.4. System controller

The block diagram of the proposed system scheme is shown in Figure 5. The power flow from the dc source to the utility is controlled by the reference current signal, which is built by the microcontroller. This signal, as can be seen in Figure 5, is a rectified unipolar sinusoidal waveform. The control scheme is used to generate the reference current signal, which is required to control power transfer and power factor. In this system, flowing in dc-link inductor current i_L is forced to follow the reference signal obtained from the current reference generator. It is regulated by switching S1 and S2 according to the reference current signal. In addition, the firing angle α is determined by the desired power factor. In this way, both the RMS value injecting current and its angle (α) with respect to grid voltage v_{grid} can be adjusted by controlling the reference current signal. Thus, the dc power can be easily tuned and transferred via the step-up transformer or directly into the utility grid at

the desired power factor. In grid-connected inverters, the current injected into the grid is mainly characterized by the inner current feedback loop. The microcontroller has been programmed to build the reference inductor current. At first, the reference sinusoidal signal synchronized with the grid voltage is generated. Then the reference current signal i_{Lref} is obtained based on internal tables such that it is shaped as a rectified unipolar sine wave and shifted by angle α with respect to grid voltage (v_{grid}). Inductor current i_L should be made to track reference inductor current i_{Lref}. To achieve this, the actual current through the inductor is sampled and compared with the reference inductor current, and then it is determined the MOSFETs should be turned on/off. The driving signal for MOSFETs is obtained by using a hysteresis current controller. The hysteresis current controller and building reference current signal are implemented in the DsPIC30F3011.

The hysteresis current controller reads actual inductor current i_L and compares it with reference inductor current i_{Lref}, and then computes the error. S1 and S2 are switched on and off at a high frequency so that the inductor current i_L is restricted within a certain tolerance band that is predetermined between $i_{Lref} - \Delta I$ and $i_{Lref} + \Delta I$ according to the error computed previously.

Thus it is obtained that the current waveform through the dc-link inductor is in the shape of a rectified sinusoidal reference current by means of switching MOSFETs. The switching frequency is a function of the hysteresis tolerance bandwidth. If the tolerance band chosen is large, the harmonic level in the injected sinusoidal current is lower but it needs high frequency switching.

Here, to track the reference inductor current the positive/negative dc-link voltage (V_a) is applied to the DC-link inductor. The hysteresis controller must define the right signals to increase or decrease the inductor current. If inductor current i_L is less than the reference inductor current ($i_{Lref} - -\Delta I$), then two MOSFETs (S1 and S2) are switched on. This means that positive voltage is applied to the DC-link inductor ($+V_a$). In this way, the inductor current is increased until reaching the maximum hysteresis band. If inductor current i_L is greater than the reference inductor current ($i_{Lref} + \Delta I$), then *S1* and *S2* are switched off. Thus, negative voltage is applied to the DC-link inductor ($-V_a$). This means that the inductor current is decreased until reaching the minimum hysteresis band.

Consequently, the inductor current i_L remains constant at the desired value by controlling the switch status. The hysteresis controller is so simple that it can be performed with a few lines of C-language program codes in DsPIC30F3011. Accordingly, it needs less computation and saves time to do other duties for the microcontroller.

4. Simulation and experimental results

4.1. Simulation results

The proposed LCI was simulated with MATLAB/Simulink. The simulation model of the proposed system has been built as shown in Figure 6. The simulation parameters are $I_{Lref} = 4$ A and 2.4 A, L = 5 mH, the resistance is included to simulate the real inductor (r = 0.4 Ω), $V_{dc} = 25.6$ V, $V_{grid} = 16.8$ V, and $f = 50$ Hz, and the tolerance band ΔI is chosen as 0.2 A in order to limit the maximum switching frequency at 10 kHz. The simulation parameters have been chosen to match experimental values. I_{Lref} denotes the reference RMS value of the injected current (I_{grid}) and it is equal to the RMS value of the reference dc-link inductor current.

In the following, simulation results are obtained using MATLAB/Simulink with the Power systems toolbox. The overall performance of the proposed inverter is simulated for two different configurations of firing angles ($\alpha = 120^\circ$ and $\alpha = 145^\circ$) and reference currents ($I_{Lref} = 2.4$ A and $I_{Lref} = 4$ A), and then detailed in the Table. Figures 7 and 8 show the simulation results.

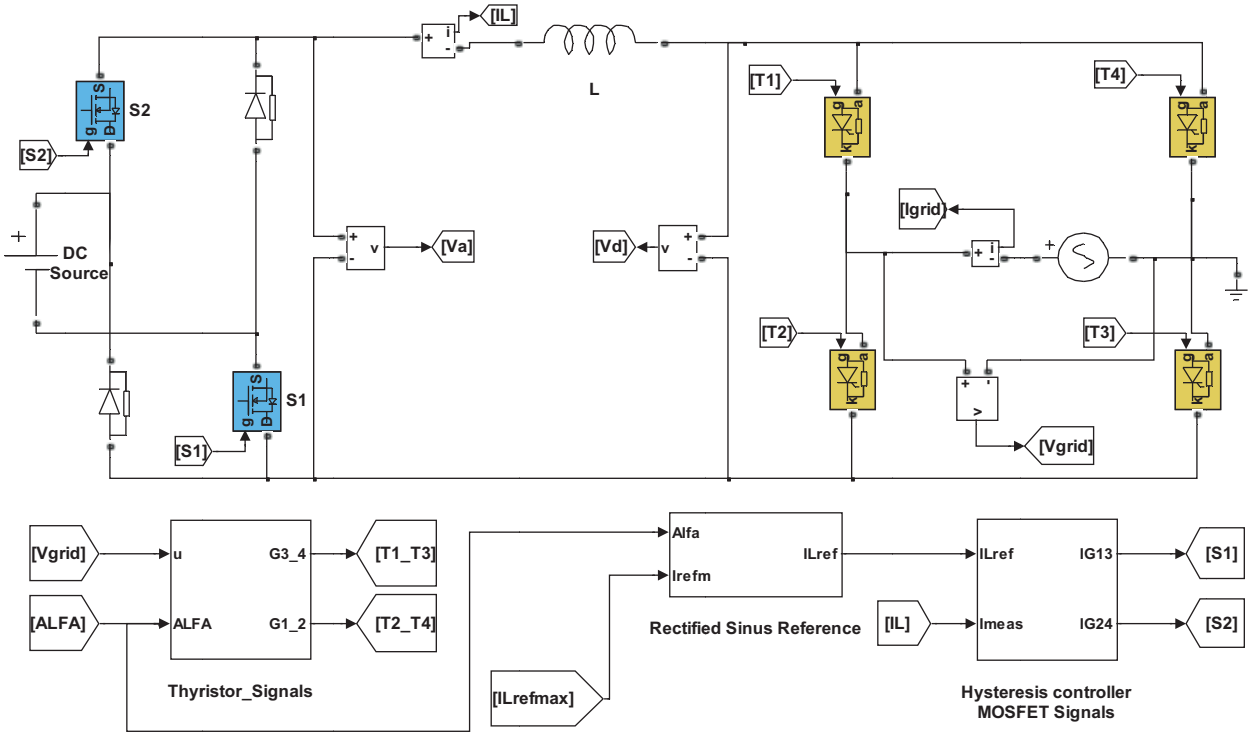

Figure 6. The simulation model of the proposed LCI system.

Table. Comparison of simulation and experimental results.

	$\alpha = 120°$			
	$I_{Lref} = 2.4$ A		$I_{Lref} = 4$ A	
	Simulation results	Experimental results	Simulation results	Experimental results
Injection current to the grid (I_{grid})	2.4 A	2.4 A	4 A	4 A
Active power transfer to the grid (P_{grid})	19.58 W	17.4 W	32.97 W	30.1 W
Active power generated from DC source (P_{dc})	25.8 W	27.6	45.68 W	47.36
Power factor ($\cos\varphi$)	0.5	0.45	0.5	0.46
Total harmonic distortion in the current (THD_i)	4.4%	4.8%	2.6%	2.73%
	$\alpha = 145°$			
	$I_{Lref} = 2.4$ A		$I_{Lref} = 4$ A	
	Simulation results	Experimental results	Simulation results	Experimental results
Injection current to the grid (I_{grid})	2.4 A	2.4 A	4 A	4 A
Active power transfer to the grid (P_{grid})	32.25 W	31.7 W	54.18 W	53.2 W
Active power generated from DC source (P_{dc})	38.16 W	40.44 W	66.9 W	68.1 W
Power factor ($\cos\varphi$)	0.819	0.78	0.819	0.79
Total harmonic distortion in the current (THD_i)	4.15%	4.9%	2.5%	2.80%

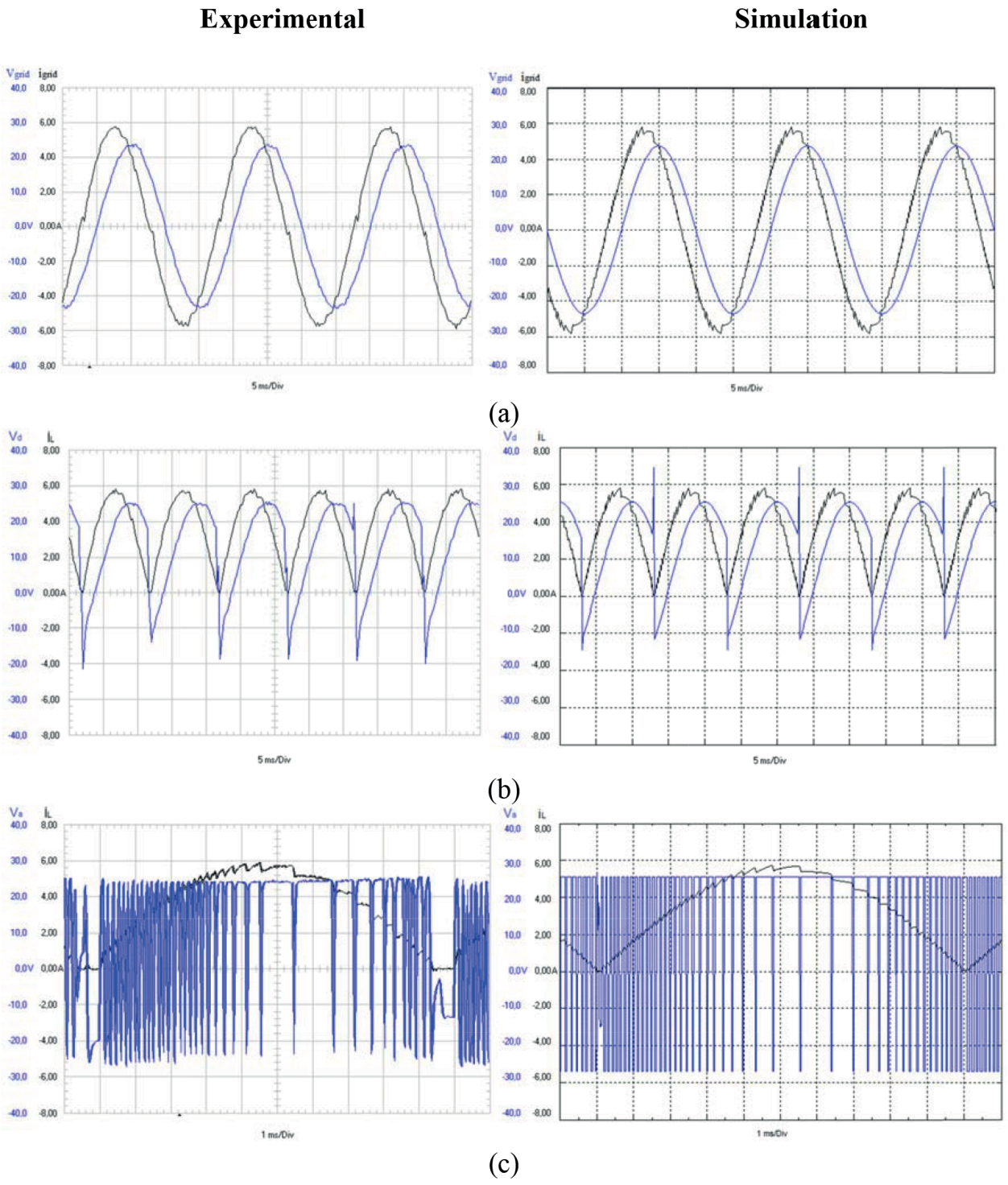

Figure 7. Experimental and simulation waveforms of the proposed inverter for $\alpha = 145^\circ$ and $I_{Lref} = 4$ A. (a) v_{grid} and i_{grid} (b) LCI module output (V_d) and inductor current (i_L), (c) sinusoidal injection module output (V_a) and i_L.

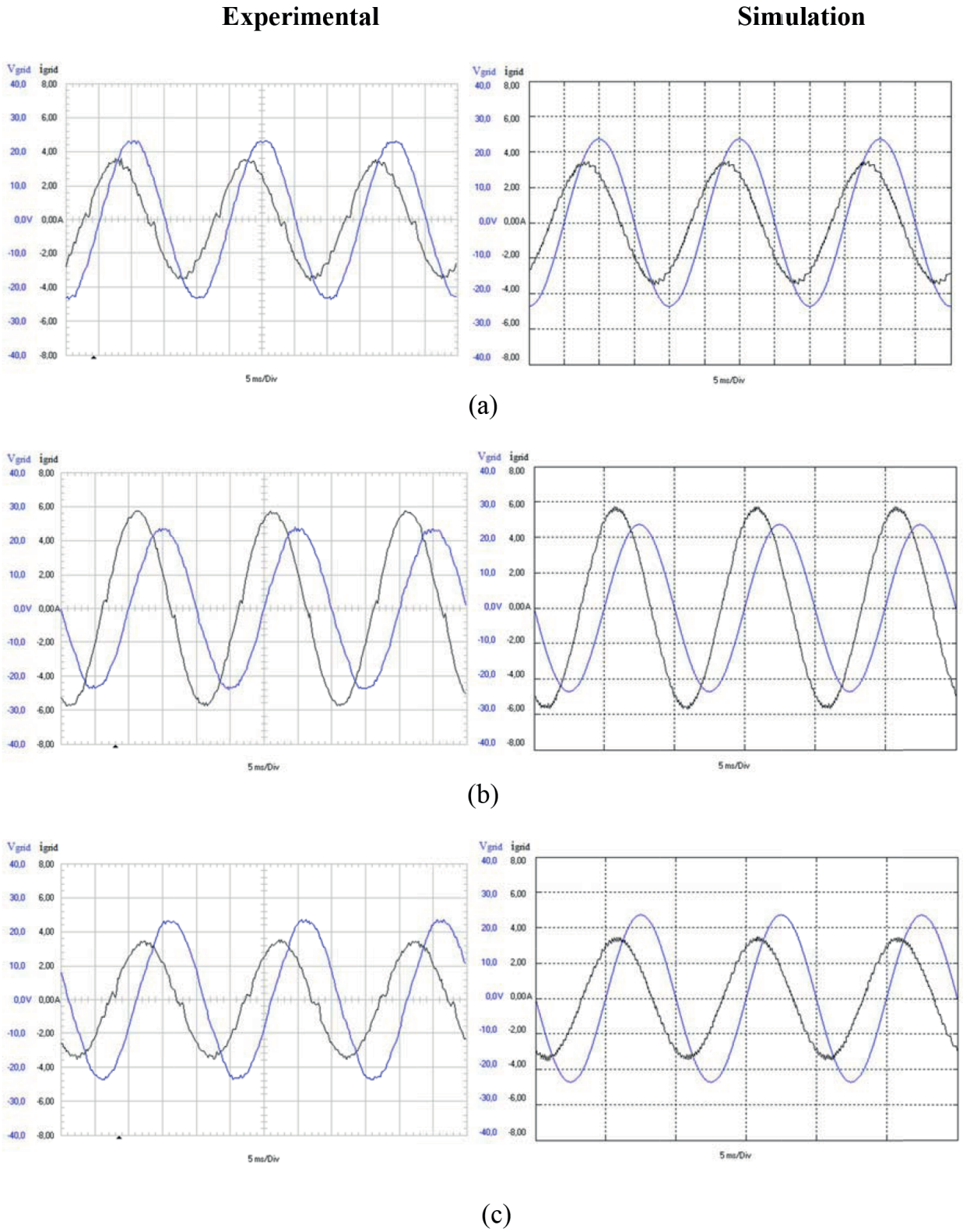

Figure 8. Experimental and simulation waveforms of the v_{grid} and i_{grid} (a) for $\alpha = 145^\circ$ and $I_{Lref} = 2.4$ A, (b) for $\alpha = 120^\circ$ and $I_{Lref} = 4$ A, (c) for $\alpha = 120^\circ$ and $I_{Lref} = 2.4$ A.

In the simulation, hysteresis controller bandwidth is chosen as the same value as the experimental value in order to have the same switching frequency in both the simulations and experimental results. For the chosen band size, the switching frequency of MOSFET is approximately around 10 kHz. This is because the digital implementation of the current control was limited to 10 kHz due to the low-speed analogue to digital converter (ADC) of the chosen microcontroller.

4.2. Experimental results

The experimental setup of the proposed system consists of a single-phase step-up transformer, a single-phase full controlled SCR bridge, a dc-link inductor, two high switches (MOSFETs) (S1 and S2), two power diodes, driving and firing circuits, and a DsPIC30F3011 controller.

A single-phase transformer (16.8/220 V) has been connected between the line-commutated inverter and the grid. The microcontroller implements the hysteresis controller and then generates driving signals for MOSFETs and firing signals for SCRs accordingly. The driving circuit has been developed to trigger the SCRs and MOSFETs as optical isolators. The firing angle of the inverter is set at two different fixed values that are chosen above 90° in order to facilitate inverter operation. The experimental results for different values of firing angles (120° and 145°) and reference currents (2.4 A and 4 A) are summarized in the Table and shown in Figures 7 and 8. It can be also seen from the Table that the simulation and experimental results are quite similar. The difference between the results can arise from impedance of the cables, calibration of the measuring devices, and simulation models of the thyristors, MOSFETs, and diodes.

The THD of the injecting current to the grid with $I_{Lref} = 4$ A and $\alpha = 145°$ is 2.8%, and is given as a harmonic spectrum in Figure 9. All of the THDs obtained for two different firing angles and reference currents are listed in the Table, which are less than 5%, and these values meet the grid-connected standards.

5. Conclusion

This paper presents a new power electronic interface for connecting to a utility grid. Owing to the proposed inverter, the dc power obtained from renewable energy sources can be transferred to the grid by providing injected current that is a high quality ac sinusoidal current, as seen in Figures 7 and 8. By this means, it eliminates ac side harmonic filters used in conventional line-commutated inverters and the harmonic cancellation technique.

This inverter also allows control of the injecting current as well as high quality in contrast to other conventional line-commutated inverters. The reference current signal is used to control power transfer from the dc source to the grid at the desired firing angle/power factor α of the LCI. Moreover, it allows operating with a controllable power factor by adjusting the firing angle. The angle α can be close to 180° and so the system should not need reactive power compensation equipment.

The proposed LCI is simulated and experimentally verified. The simulation and experimental results are quite similar and they both show good performance of the proposed topology that is far better than that of the conventional line-commutated inverter. The proposed method eliminates the problems of harmonics in the ac current injected into the grid owing to the sinusoidal current injection module. The results show that without any harmonic compensation the THD of injected current is less than 5% even in low power operation. As seen from the simulation and experimental results in the Table, the higher grid current waveform is closer to pure sinusoidal with lower harmonic contents. Therefore, the THD_i would be close to zero at higher power.

The simulation and experimental results confirm that the proposed inverter satisfies IEEE 1547 and IEC 61727 requirements. In this paper a 50-Hz step-up transformer (16.8/220 V) is used for the laboratory

prototype to allow studying lower power in the laboratory. It can be seen from the Table that the relatively low efficiency of the inverter is partly due to the low output voltage of the prototype. Increasing the output voltage will correspondingly reduce the effect of the voltage drop of the components. In future work it is proposed to address the above efficiency to examine the scaling of the proposed topology to higher voltage levels. Therefore, the step-up transformer can be eliminated by providing a large dc source at the dc side. Hence, the number of stages in such systems can be reduced. The proposed single-phase LCI inverter topology is a good alternative to power transfer from renewable energy sources (photovoltaic, fuel cell etc.) to the utility grid.

Acknowledgment

This work is supported by the Scientific Research Projects Unit of Kocaeli University (grant no. 087-2010).

References

[1] Mohan N, Undeland T, Robbins W. Power Electronics: Converters Applications and Design. 3rd ed. New York, NY, USA: Wiley, 2003.

[2] Rashid MH. Power Electronics Handbook. 2nd ed. San Diego, CA, USA: Academic Press, 2001.

[3] Sahan B, Araujo S, No?ding C, Zacharias P. Comparative evaluation of three-phase current source inverters for grid interfacing of distributed and renewable energy systems. IEEE T Power Electr 2011; 26: 2304-2318.

[4] Kjaer SB, Pederson JK, Blaabjerg F. A review of single-phase grid-connected inverters for photovoltaic modules. IEEE T Ind Appl 2005; 41: 1292-1306.

[5] Calais M, Myrzik J, Spooner T, Agelidis VG. Inverters for single-phase grid connected PV systems: an overview. In: IEEE 2002 Power Electronics Specialists Conference; 23–27 June 2002; Cairns, Australia: IEEE. pp. 1995-2000.

[6] IEEE 1547.2-2008. IEEE Standard for interconnecting distributed resources with electric power systems. 2009; 1-217.

[7] Sick F, Erge T. Photovoltaics in Buildings. XYZ Publishing Company, 1995.

[8] Al-Nasseri H, Redfern MA. Solid-state converter topologies for interfacing DC sources with utility power systems. In: IEEE 2004 Universities Power Engineering Conference; 6–8 Sept. 2004; Bristol, UK: IEEE. pp. 629-633.

[9] Lavanya V, Gounden NA, Rao PM. A simple controller using line commutated inverter with maximum power tracking for wind-driven grid-connected permanent magnet synchronous generators. In: IEEE 2006 Power Electronics, Drives and Energy Systems; 12–15 Dec 2006; New Delhi, India: IEEE. pp. 1-6.

[10] Shanthi T, Gounden NA. Power electronic interface for grid-connected PV array using boost converter and line-commutated inverter with MPPT. In: IEEE 2007 Intelligent & Advanced Systems; 25–28 Nov 2007; Kuala Lumpur, Malaysia: IEEE. pp. 882-886.

[11] Arjun A, Vinod B, Kumaresan N, Jose DRBB. A power electronic controller for PV-tied grid-connected system with single parameter sensing for mppt using boost converter and line-commutated inverter. In: IEEE 2012 System Engineering and Technology; 11–12 Sept 2012; Kathmandu, Nepal: IEEE. pp. 36-40.

[12] Gounden NGA, Peter SA, Nallandula H, Krithiga S. Fuzzy logic controller with MPPT using line-commutated inverter for three-phase grid-connected photovoltaic systems. Renew Energ 2009; 34: 909-915.

[13] Pilli VPB, Bhamu M. Power electronic interface for grid-connected PV array using SEPIC converter and line-commutated inverter with MPPT. International Journal of Engineering Research & Technology 2013; 2: 1-6.

[14] Krithiga S, Gounden NGA. Power electronic configuration for the operation of PV system in combined grid-connected and stand-alone modes. IET Power Electronics 2014; 7: 640-647.

[15] IEC Standard 61727. Characteristic of the utility interface for photovoltaic (PV) systems. 2002.

[16] Enslin JHR, Heskes PJM. Harmonic interaction between a large number of distributed power inverters and the distribution network. IEEE T Power Electr 2004; 19: 1586-1593.